WILEY-VCH

Peptide Nanomaterials Designed from Natural Supramolecular Systems

Hiroshi Inaba and Kazunori Matsuura*[a,b]

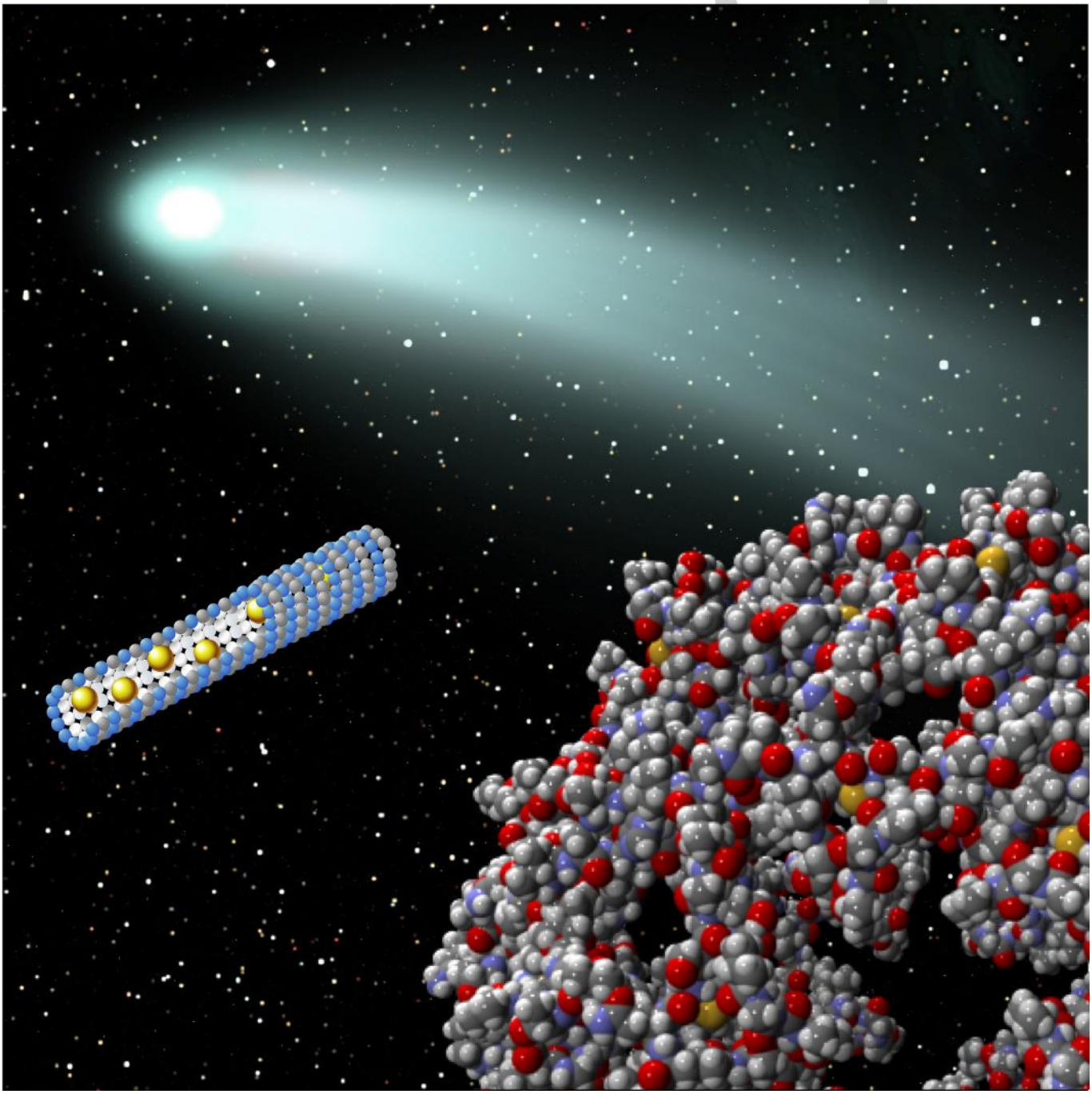

Abstract: Natural supramolecular assemblies exhibit unique structural and functional properties that have been optimized over the course of evolution. Inspired by these natural systems, various bio-nanomaterials have been developed using peptides, proteins, and nucleic acids as components. Peptides are attractive building blocks because they enable the important domains of natural protein assemblies to be isolated and optimized while retaining the original structures and functions. Furthermore, the peptide subunits can be conjugated with exogenous molecules such as peptides, proteins, nucleic acids, and metal nanoparticles to generate advanced functions. In this personal account, we summarize recent progress in the construction of peptide-based nanomaterial designed from natural supramolecular systems, including (1) artificial viral capsids, (2) self-assembled nanofibers, and (3) protein-binding motifs. The peptides inspired by nature should provide new design principles for bio-nanomaterials.

1. Introduction

Natural supramolecular assemblies such as microtubules, actin filaments, clathrin, chromatin, ribosomes, and viruses have unique structural and functional properties that have been optimized over the course of evolution.[1] To perform their roles in organisms correctly, the supramolecular assemblies form homogeneous structures with defined size and morphology, structural rigidity/flexibility, dynamic structural change, and selective interaction with target molecules. The sophisticated and elaborate systems in nature have inspired scientists to mimic the natural supramolecular assemblies to construct bioinspired and biomimetic nanomaterials. Various biomolecules including peptides,[2-12] proteins,[12-15] and DNA[16-20] have been utilized as building blocks for this purpose. Peptides in particular are ideal building blocks because of the high designability using natural and non-natural amino acids, self-assembly, and molecular recognition capability. The high affinity of peptides to target molecules can be used to create hybrid nanomaterials consisting of peptides and organic/inorganic materials such as metal nanoparticles and polymers.[21] Importantly, naturally derived peptides that are extracted and rationally designed from the parts of natural proteins potentially retain their original functions, such as structural scaffolding, self-assembling, and molecular recognition capabilities.[22,23] For instance, widely studied cell adhesion motifs such as RGD and IKVAV are derived from the adhesion proteins fibronectin and laminin, respectively.[22] Based on the unique properties of peptides, various peptide nanomaterials have been fabricated, including nano- and microarchitecture such as spheres, fibers, and tubes;[7-12] stimulus-responsive materials;[24] catalytic assemblies;[25] and metal-binding peptide assemblies.[5] This personal account provides a comprehensive overview of the recent design of peptide nanomaterials based on natural supramolecular systems, developed by our and other groups. We focus on three types of peptide nanomaterial: artificial viral capsids, nanofibers, and protein-binding peptides. Artificial viral capsids with nanosphere structures were developed inspired by natural viral scaffolds (Figure 1a). Spatiotemporal modulation of peptide nanofiber growth was developed and applied to create self-propelled systems by mimicking natural actin filament growth ("actin comet tail") (Figure 1b). Moreover, microtubule-binding peptides were designed from a natural microtubule-binding protein (Figure 1c). These peptide-based systems that mimic and surpass the equivalent natural functions provide design principles for the next generation of peptide-based nanomaterials.

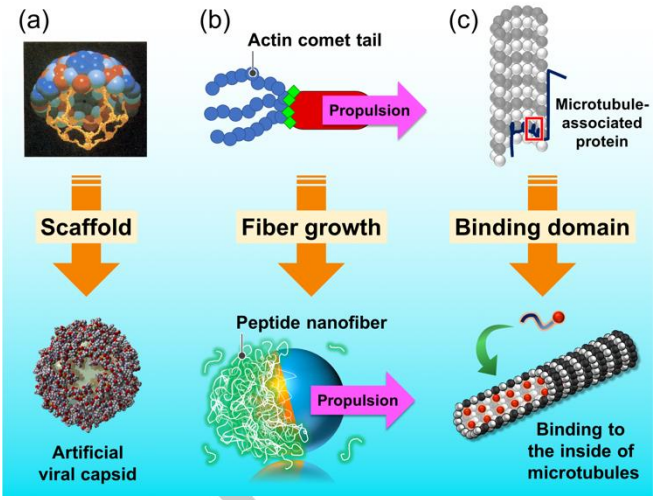

Figure 1. Examples of peptide-based nanomaterials designed from natural supramolecular systems: (a) virus-inspired artificial viral capsid, (b) spatiotemporal peptide nanofiber growth for propulsion of giant liposome inspired by actin comet tail, and (c) microtubule-binding peptide designed from microtubule-associated protein.

[a] Dr. H. Inaba, Prof. Dr. K. Matsuura
Department of Chemistry and Biotechnology
Graduate School of Engineering, Tottori University
Koyama-Minami 4-101, Tottori 680-8552 (Japan)
E-mail: ma2ra-k@tottori-u.ac.jp
[b] Dr. H. Inaba, Prof. Dr. K. Matsuura
Centre for Research on Green Sustainable Chemistry, Tottori University

Hiroshi Inaba obtained his Ph.D. from Kyoto University in 2015. During his Ph.D., he worked as Research Fellow of the Japan Society for the Promotion of Science (JSPS) for Young Scientists at the Institute for Integrated Cell-Material Sciences (iCeMS), Kyoto University. In 2015, he joined the Department of Chemistry at University of Illinois Urbana-Champaign as a postdoctoral research associate. Since 2016, he has been working as an Assistant Professor at the Department of Chemistry and Biotechnology at Tottori University.

Kazunori Matsuura obtained his Ph.D. from Tokyo Institute of Technology in 1996 and then joined the Department of Molecular Design and Engineering at Nagoya University as an Assistant Professor. In 2001, he moved to the Department of Chemistry and Biochemistry at Kyushu University, where he served as an Associate Professor. In 2006, he was selected as a researcher for the JST PRESTO project "Structure Control and Function." Since 2012, he has been working as a Full Professor at the Department of Chemistry and Biotechnology at Tottori University. Prof. Matsuura received The Young Scientists' Prize from the Minister of Education, Culture, Sports, Science and Technology in 2008, the JSPS Prize from the Japan Society of the Promotion of Science in 2012, and The Chemical Society of Japan Award for Creative Work in 2016.

2. Self-assembled Artificial Viral Capsids

Viruses are natural forms of nanoarchitecture consisting of coat proteins (capsids) and nucleic acids. Since viruses form rigid, highly stable, homogeneous, and highly symmetric nanostructures for efficient infection into host cells, scientists have engineered viruses for the fabrication of nanomaterials. Since viral capsids self-assemble to form virus-like particles (VLPs) even after removing the genomes, VLPs have been used as templates for the construction of nanocarriers, nanoreactors, and nanodevices. Various types of virus and VLP derived from spherical (e.g., cowpea chlorotic mottle virus, cowpea mosaic virus), rod-like (e.g., tobacco mosaic virus, bacteriophage M13), and tailed (e.g., bacteriophage T4) viruses have been utilized for bio-nanotechnology applications.[26-36] Inspired by VLPs based on natural viruses, artificial viral capsids (AVCs) that are self-assembled nanostructures with virus-like dimensions and morphology have been developed. AVCs with the desired size and morphology have been developed by rational design of the self-assembly of peptides and proteins.[31,37-40] For instance, protein-based AVCs with hollow capsule structures have been constructed by designing the protein subunits based on the geometric parameters of polyhedra.[41-45] In this section, recent developments of peptide-based AVCs by our group and others are described.

2.1. Virus-like Nanospheres Formed by Self-assembly of Trigonal Peptides

Inspired by natural spherical viruses and clathrin lattices in which the spherical nanostructures are formed by using triskelion structures as building blocks, spherical AVCs based on trigonal peptides have been developed by our group[46-50] and others.[51-53] In 2005, we reported a first example of the self-assembly of C_3-symmetric Trigonal(FKFE)$_2$ containing a β-sheet-forming peptide FKFEFKFE to a spherical AVC (Figure 2a).[46] Trigonal(FKFE)$_2$ forms anti-parallel β-sheet structures by intermolecular interactions, which results in self-assembly to form spherical structures. The formation of nanospheres was observed by atomic force microscopy (AFM), showing diameters of 35–70 nm, and by scanning electron microscopy (SEM), showing diameters of 22–34 nm. The molecular model shows that the distance between the core benzene rings of two Trigonal(FKFE)$_2$ molecules is ca. 5.8 nm when an anti-parallel β-sheet is formed. From this distance, the average diameter of the dodecahedron structure formed by the self-assembly of Trigonal(FKFE)$_2$ is estimated to be ca. 16 nm. The estimated diameter is in good agreement with the average diameter of the nanospheres (19.1 ± 4.0 nm) observed by dynamic light scattering (DLS). Thus, the C_3-symmetric strategy is useful to construct spherical AVCs by designing self-assembled peptide units.

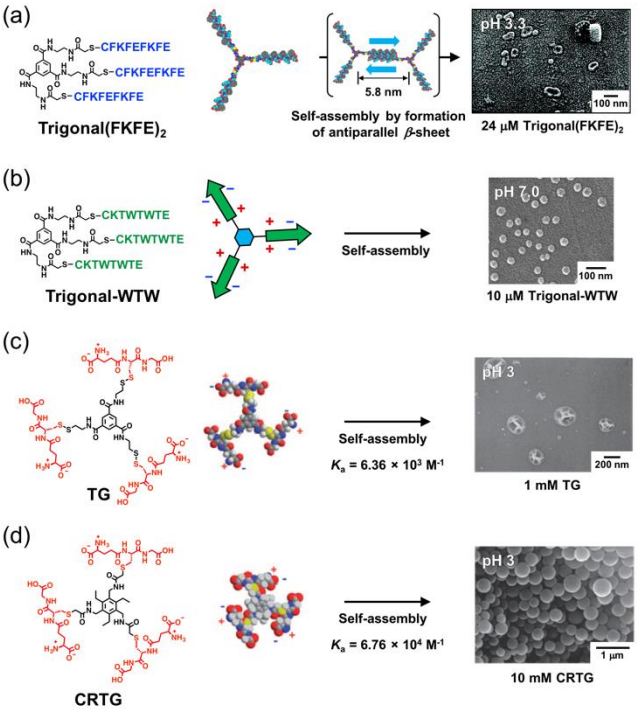

Figure 2. Construction of AVCs by self-assembly of trigonal peptides and SEM images of the resulting assemblies. (a) Trigonal(FKFE)$_2$. Adapted with permission from ref. 46. Copyright 2005 American Chemical Society. (b) Trigonal-WTW. Adapted with permission from ref. 47. Copyright 2011 Royal Society of Chemistry. (c) Trigonal-glutathione (TG). Adapted with permission from ref. 48. Copyright 2009 Royal Society of Chemistry. (d) Conformation-regulated trigonal-glutathione (CRTG). Adapted with permission from ref. 50. Copyright 2010 Chemical Society of Japan.

We applied the C_3-symmetric strategy to construct spherical AVCs by using a tryptophan zipper-forming peptide CKTWTWTE (Trigonal-WTW) (Figure 2b).[47] Trigonal-WTW self-assembled to form nanosphere structures at pH 7.0, as observed by SEM. When the pH was changed, irregular aggregates (pH 3.0) and a mixture of spherical assemblies and fibrous assemblies (pH 11) were observed. The pH dependence of the self-assembled structure of Trigonal-WTW could be ascribed to changes in peptide charges at different pH levels. Since the isoelectric point (*pI*) of Trigonal-WTW is estimated to be 7.1, it possesses a zwitterionic structure at pH 7. Trigonal-WTW forms nanospheres by forming intermolecular antiparallel β-sheet-like structures (including tryptophan zipper) due to the attractive ionic complementarity. Thus, the unique self-assembly property of Trigonal-WTW is due to the C_3-symmetric structure and tryptophan zipper structure.

A simple tripeptide motif glutathione has also been utilized for the construction of nanospheres.[48-50] Trigonal conjugation of glutathione (Trigonal-glutathione, TG) formed spherical assemblies with sizes of 100–250 nm in water (Figure 2c).[48] The size and morphology of the TG assemblies were minimally affected at pH 3–7, indicating the high stability of the nanospheres. ^{1}H-NMR chemical shifts revealed that TG is self-assembled by interactions between glutathione units (hydrogen bonding, electrostatic interactions) with an apparent association constant of K_a = 6.36 × 10^3 M^{-1}. The nanospheres were shown to change structure from hollow to filled spheres depending on the concentration. At lower concentrations (0.1 and 1.0 mM), wrinkly collapsed or dehydrated assemblies on a carbon-coated grid were observed by SEM (Figure 2c), indicating the hollowness of the nanostructures. In contrast, hard spheres were observed at a higher concentration of 10 mM, suggesting the existence of filled spheres. A guest molecule, uranine, was encapsulated into the TG nanospheres only at lower concentrations of TG, supporting our assumption that the assemblies of TG possess hollow structures at lower concentrations. Controlled release of guest molecules from TG nanospheres was carried out by reduction using dithiothreitol.[49] By the addition of dithiothreitol, the recombination of disulfide bonds of the guest-encapsulated TG nanospheres occurred, resulting in the gradual release of guest molecules. In a similar strategy, we constructed a trigonal composite, CRTG, consisting of glutathiones having a 1,3,5-tris(aminomethyl)-2,4,6-triethylbenzene core (Figure 2d).[50] Self-assembly of CRTG results in the formation of hard spherical structures with sizes of 310 ± 50 nm at pH 3. The CRTG assemblies gradually collapsed upon increasing pH from 3 to 10. Since the *pI* of CRTG is estimated to be 2.9, the disruption of the spherical assemble at higher pH would be due to the electrostatic repulsion between glutathione units of CRTG. The hard and regular morphology at pH 3 contrasting with that of the TG nanospheres is ascribed to the difference of benzene core. Three glutathione units of CRTG are conformationally regulated due to the steric repulsions between the ethyl groups attached to the benzene core, resulting in the hard and regular nanosphere structures.

2-2. Artificial Viral Capsids by Self-assembly of β-Annulus Peptides

Extraction of self-assembly motifs from natural spherical viruses is a novel and promising strategy for constructing peptide-based spherical AVCs. Since many spherical viruses have a trimeric annular β-structure called a "β-annulus motif" as a self-assembly motif, we developed AVCs based on the β-annulus motifs of spherical viruses.[54,55] TBSV consists of 180 quasi-equivalent protein subunits containing 388 amino acids each to form a capsid of ca. 33 nm in diameter (Figure 3a).[56-58] In 2010, we developed a 24-mer β-annulus peptide (INHVGGTGGAIMAPVAVTRQLVGS) of tomato bushy stunt virus (TBSV), which self-assembles to form a hollow nanocapsule (β-annulus capsid) in water (Figure 3b).[54] Spherical assemblies with 30–50 nm in diameter were observed by transmission electron microscopy (TEM) (Figure 3c) and the

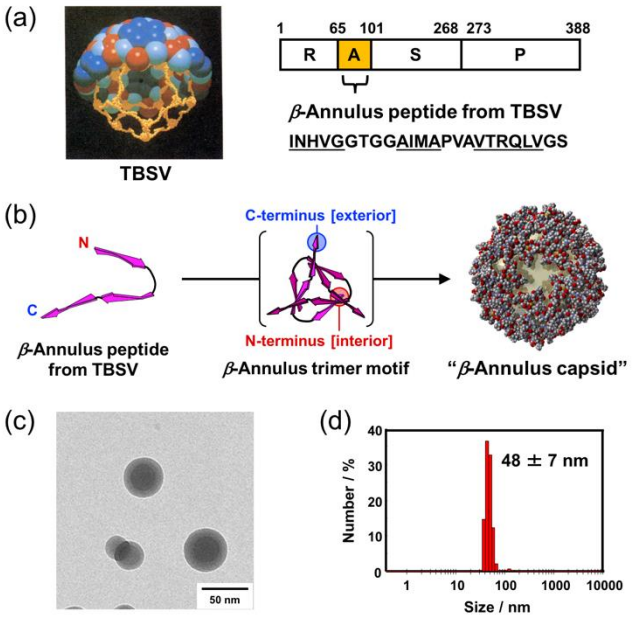

Figure 3. Formation of artificial viral capsid by self-assembly of β-annulus peptide designed from tomato bushy stunt virus (TBSV). (a) Quaternary structure of TBSV showing the internal framework in orange. Bar diagram of subunit of TBSV consisting of the R-(RNA-binding) domain, A-(β-annulus and extended arm) domain, S-(shell) domain, and P-(projection) domain. (b) Self-assembly of β-annulus peptide from TBSV (Ile69–Ser92) to form β-annulus capsid. (c) TEM image and (d) DLS of the β-annulus capsid. Adapted with permission from refs. 56 and 54. Copyright 1983 Elsevier and 2010 John Wiley and Sons, respectively.

hydrophobic diameter of the assemblies was 48 ± 7 nm, as determined by DLS (Figure 3d). The synchrotron small-angle X-ray scattering (SAXS) profile indicates the existence of a hollow interior space of the β-annulus capsid. The critical aggregation concentration (CAC) of β-annulus capsid is 25 μM, and the size of β-annulus capsid is not affected by peptide concentrations above CAC. The subsequent study of pH-dependent ζ-potential measurement revealed that the N- and C-termini of the β-annulus peptide are directed to the interior and exterior of the β-annulus capsid, respectively.[59] According to this information, we established a design of molecular encapsulation inside the β-annulus capsid and molecular decoration on its exterior, as described in the following sections.

2-2-1. Molecular Encapsulation Inside β-Annulus Capsids

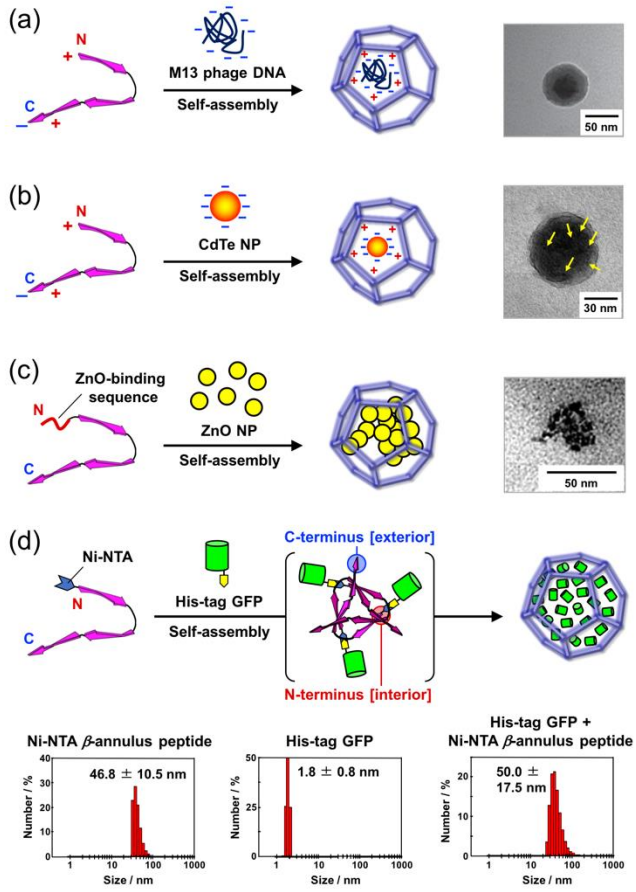

Figure 4. Encapsulation of guest molecules in the β-annulus capsids. (a) Encapsulation of M13 phage DNA. Adapted with permission from ref. 59. Copyright 2013 Springer Nature. (b) Encapsulation of anionic CdTe quantum dots. Arrow indicates the position of CdTe quantum dots. Adapted with permission from ref. 60. Copyright 2016 Chemical Society of Japan. (c) Encapsulation of ZnO NPs using ZnO-binding sequence. Adapted with permission from ref. 61. (d) (Top) Conjugation of His-tag GFP to the Ni-NTA-modified β-annulus peptide and formation of the GFP-encapsulated capsid. (Bottom) Size distribution obtained from DLS of Ni-NTA-modified β-annulus peptide (left), His-tag GFP (middle), and equimolar mixture of His-tag GFP and Ni-NTA-modified β-annulus peptide (right). Adapted with permission from ref. 62. Copyright 2016 Royal Society of Chemistry.

The hollow internal space of the β-annulus capsid has been utilized to encapsulate various guest molecules by simple electrostatic interaction or conjugation with guest-binding peptides to the β-annulus peptide.[59-62] Since the cationic N-terminal region of the β-annulus peptide is directed to the interior surface, the anionic dyes were efficiently encapsulated in the capsid, in contrast to cationic dyes.[59] Large M13 phage DNA (7249 bp) was also successfully encapsulated in the β-annulus capsid (Figure 4a).[59] The encapsulation of the M13 phage DNA was achieved at pH 4.3 because the capsid has a cationic interior and zwitterionic surface at this pH. When the DNA-encapsulated capsids were stained with uranyl acetate and cisplatin (for DNA staining), core-shell nanospheres with a diameter of 95 ± 13 nm were observed by TEM (Figure 4a). This size is similar to that obtained from the DLS (82 ± 17 nm). The size of the DNA-encapsulated capsids was larger than that of the only β-annulus capsid (48 ± 7 nm by DLS). Thus, the encapsulation of large DNA was achieved by the dynamic morphological change of the β-annulus capsid, resulting in the formation of the core-shell nanospheres.

Encapsulation of anionic CdTe quantum dots (3 nm) into the β-annulus capsid was achieved by a method similar to that for the DNA encapsulation (Figure 4b).[60] The TEM image of CdTe quantum dots in the presence of the β-annulus peptide showed that the nanospheres overlapped with CdTe quantum dots, suggesting the encapsulation of the quantum dots in the β-annulus capsid. The encapsulation behavior was analyzed by fluorescence correlation spectroscopy (FCS). The FCS curves of a mixture of CdTe NPs and the β-annulus peptide at concentrations above the CAC were fitted with a dual-component model, indicating the coexistence of free and encapsulated CdTe NPs. The apparent diameters of the slow component appearing above the CAC were estimated to be about 30–50 nm, which is similar to the diameter of the capsid.

Because the N-terminus of the β-annulus peptide is located on the interior surface of the capsid, binding motifs can be fused to the N-terminus for the encapsulation of specific guest molecules. A ZnO-binding sequence (HCVAHR) was fused to the N-terminus of β-annulus peptide through a flexible linker (GGG) for the encapsulation of ZnO NPs (Figure 4c).[61] By incubation of the ZnO-binding peptide with ZnO NPs (individual size: ~10 nm), the assembled structures of several ZnO NPs were observed by TEM. DLS showed that the average size of the complex was 48 ± 24 nm, corresponding to the TEM results. Since only ZnO-binding peptide or unmodified β-annulus peptide, which lacks the ZnO-binding sequence, formed large aggregates upon mixing with ZnO NPs, the 50-nm assembly of several ZnO NPs was formed specifically via encapsulation by the ZnO-binding β-annulus capsid.

By a similar strategy, His-tag GFP was encapsulated in the capsid by the insertion of Ni-NTA (nitrilotriacetic acid) into the N-terminus of the β-annulus peptide (Figure 4d, upper).[62] The Ni-NTA-modified β-annulus peptide retained the self-assembly capability to form the capsid with 46.8 ± 10.5 nm diameter (Figure 4d, bottom). By size exclusion chromatography (SEC), 91% encapsulation of His-tag GFP in the capsid was detected, whereas only 9% of His-tag GFP was nonspecifically bound to the unmodified β-annulus peptide lacking the Ni-NTA moiety. DLS showed that the GFP-encapsulated capsid had an average size with 50.0 ± 17.5 nm, indicating that the encapsulation had a minimal effect on the capsid size.

These results indicate that encapsulation of various guest molecules including DNA, metal NPs, and proteins in the β-annulus capsid can be achieved by simple electrostatic interaction and N-terminal modification. The encapsulation methodology is useful to deliver molecular cargo without affecting the exterior surface of the β-annulus capsids.

2-2-2. Decoration of the Outer Surface of β-Annulus Capsids

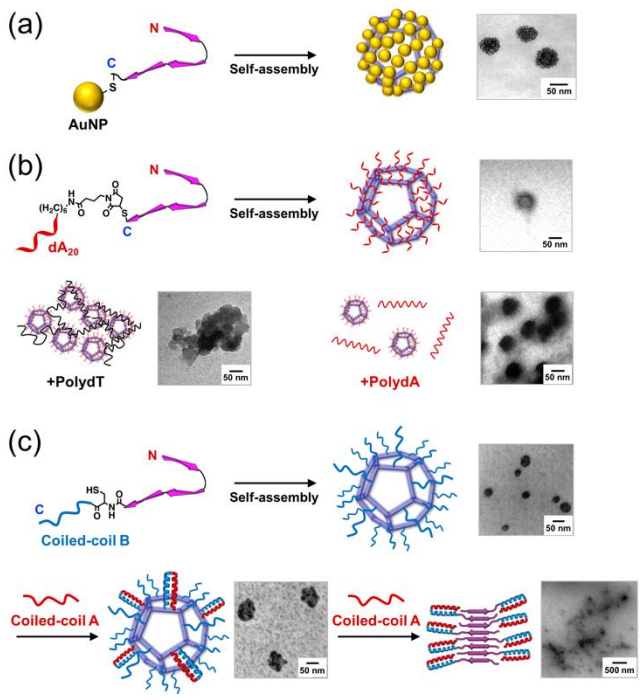

Figure 5. Decoration of exogenous molecules on the outer surface of the β-annulus capsids and TEM images of the resulting assemblies. (a) Decoration of AuNPs. (b) Decoration of dA_{20} and reaction with polydT or polydA. (c) Decoration of coiled-coil B and subsequent conjugation with coiled-coil A. Adapted with permission from refs. 63, 64, and 65. Copyright 2015 Springer Nature, 2017 John Wiley and Sons, and 2017 Royal Society of Chemistry, respectively.

Since the C-terminus of the β-annulus peptide is expected to be exposed on the outer surface when the capsid is formed,[59] various binding motifs were introduced into the C-terminus of the β-annulus peptide for decoration of the outer surface with exogenous molecules. Decoration of gold nanoparticles (AuNPs) on the capsid was achieved by the construction of a AuNP– β-annulus peptide conjugate (Figure 5a).[63] A β-annulus peptide possessing GGGCG at the C-terminus was conjugated with AuNPs (5 nm) via thiol–gold interaction at concentrations below CAC. By concentration of the conjugate, the assembled structures of AuNPs with 30–60 nm diameter were formed as observed by TEM and DLS. The ζ-potential of the AuNP–capsid composite was −30.5 ± 9.8 mV at pH 4.6, whereas the value of unmodified capsid was 0.01 ± 3.43 mV. These results indicate that the AuNPs were decorated on the outer surface of the capsid, not encapsulated inside it.

Surface decoration of single-stranded DNAs on the capsid was achieved by chemical conjugation of the DNAs to the C-terminus of the β-annulus peptide (Figure 5b).[64] DNAs (dA_{20} and dT_{20}) modified with maleimide moiety were reacted with the cysteine introduced to the C-terminus of the β-annulus peptide. The DNA-peptide conjugates were self-assembled to the capsid structures, as observed by TEM and DLS. By incubation with complementary polynucleotide (polydT to dA_{20}-modified β-annulus), the dA_{20}-modified capsid was aggregated by DNA hybridization. In contrast, the aggregation was not observed when non-complementary polydA was added to the dA_{20}-modified capsid. The same results were obtained when the dT_{20}-modified capsid was used. These results indicate that the decorated DNAs on the capsid retain the ability to recognize the complementary DNAs.

For the purpose of mimicking natural viruses such as adenovirus and influenza virus that possess coiled-coil motifs on the surface, complementary dimeric coiled-coils (coiled-coil A and coiled-coil B) were decorated on the capsid (Figure 5c).[65] First, coiled-coil B was conjugated to the C-terminus of the β-annulus peptide by native chemical ligation. The coiled-coil B-decorated β-annulus peptide self-assembled to form spherical structures of ~50 nm in diameter, as observed by TEM and DLS. By the addition of 0.2 equivalent coiled-coil A to the coiled-coil B-decorated capsid, the formation of coiled-coil structures was shown by circular dichroism (CD) measurement with the retention of spherical structures. On the other hand, when one equivalent coiled-coil A was incubated with the coiled-coil B-decorated capsid, the capsid was decomposed to form the fibrous assembly.

The above examples indicate that the surface of the β-annulus capsid can be conjugated with various materials such as metal NPs, DNAs, and peptides. Notably, the surface-decorated molecules can be utilized to recognize the target molecules such as receptor proteins, antibodies, and DNAs.

2-3. Other Design of Peptide-based Artificial Viral Capsids

Recently, functional AVCs were developed based on the rational design of peptides. A novel example is synthetic analogs derived from the transmembrane domains of the membrane protein CXCR4 (Figure 6a).[66] The 24-residue peptide from the second transmembrane helix of CXCR4 self-assembled to form ~6-nm uniform spherical nanoparticles. NMR studies suggested that the peptide monomer formed a β-hairpin-like conformation and the hairpin conformation was retained in the nanoparticles. Interestingly, the nanoparticles retained the innate biological activity of CXCR4, such as binding to cell membranes and inhibition of tumor metastasis. Successful encapsulation of hydrophobic drugs in the nanoparticles indicates that the system could be used as an efficient delivery system with the natural biological activity of CXCR4.

De novo design of coiled-coil peptides is a useful methodology to construct self-assembled AVCs because of our deep understanding of the principles for specific interaction pairs.[67-71] For instance, Ryadnov et al. developed dendrimeric virus-like assembly based on a self-complementary coiled-coil subunit having three interfacial facets (Figure 6b).[71] The coiled-coil dimer with a disulfide bond self-assembled to form 12-nm monodisperse spherical shells. Encapsulation of siRNA and plasmid DNA in the shells was achieved to promote gene silencing and expression, respectively. The designability of the coiled-coil peptides has great potential for creating nanostructures with defined sizes and functionalities.

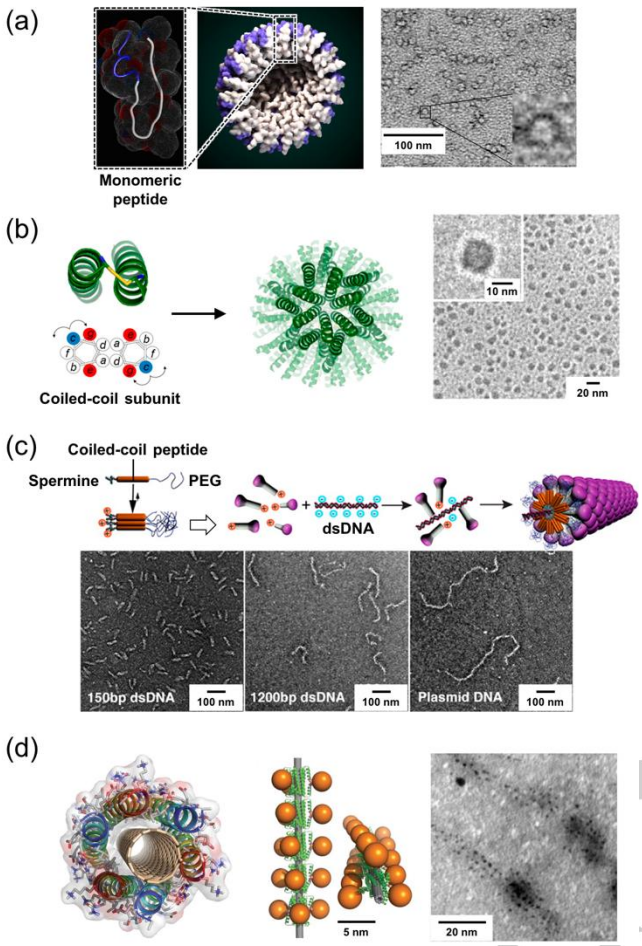

Figure 6. Peptide-based functional AVCs and TEM images. (a) Self-assembly of transmembrane domain of CXCR4 to form spherical nanoparticles. Adapted with permission from ref. 66. Copyright 2011 National Academy of Sciences, U.S.A. (b) Self-assembly of coiled-coil peptide to form the dendrimeric assembly. Adapted with permission from ref. 71. Copyright 2016 American Chemical Society. (c) DNA-templated assembly of coiled-coil peptide for construction of filamentous assembly. Adapted with permission from ref. 72. Copyright 2013 American Chemical Society. (d) Binding of modeled peptide with SWNT (left), computational model structure (center), and a TEM image (right) of gold nanoparticles grown on Cys-modified peptide wrapped around SWNTs. Adapted with permission from ref. 73. Copyright 2011 American Association for the Advancement of Science.

The construction of non-spherical AVCs such as filamentous and rod-like assemblies is challenging because of the involvement of anisotropic structures with low symmetry. Inspired by natural filamentous viruses such as tobacco mosaic virus (TMV), which uses RNA as a template for the assembly of capsids, homogeneous 1D nanostructures have been constructed by using DNA and carbon nanotubes as templates for the assembly of peptide units.[72,73] Stupp et al. designed a coiled-coil peptide conjugated with a PEG chain at one terminus and a cationic spermine unit (DNA-binding domain) at the other (Figure 6c).[72] By templating with linear or circular double-stranded DNAs, the pre-assembled mushroom-shaped nanostructures self-assembled to form filamentous complexes. The length of the filaments was dependent on the length of the template DNA. DeGrado et al. reported an elegant computational design of helical peptide motifs that specifically assemble into a virus-like tubular structure surrounding single-walled carbon nanotubes (SWNTs) (Figure 6d).[73] Coiled-coil peptides containing Ala or Gly residues as sites contacting SWNTs were computationally optimized to adhere to the periodic carbon atoms in SWNTs. The resulting peptides wrapped hydrophobic SWNTs to form water-soluble SWNT–peptide assemblies. By the introduction of a cysteine to the peptide as a gold binding site, plasmonic alignment of AuNPs was formed on SWNTs.

3. Self-assembled Peptide Nanofibers

3.1. Design of Peptide-based Nanofibers

Nanofiber structures are widely observed in natural systems, such as silk, collagen, amyloid, viruses, and cytoskeleton. For instance, natural amyloid proteins such as amyloid-β peptide (Aβ) and tau protein form similar fibrous assemblies that consist of β-sheet-rich sequences.[8] Inspired by the natural fibers that are formed by the self-assembly of building block units, artificial peptide nanofibers have been developed for various applications in the fields of biomedicine, tissue engineering, renewable energy, environmental science, nanotechnology, and material science.[9,11,25,74-83] Advantages of the peptide-based nanofibers compared with other polymeric nanofibers include that (1) the nanofiber-forming peptide units are known and can be chemically tuned, and (2) stimulus-responsive groups can be introduced to the peptide moiety to control the structures of the nanofibers. The peptide nanofibers can be categorized into several groups, such as amyloid-like structures, β-sheet peptides with alternating hydrophilic and hydrophobic amino acids, peptide-synthetic hybrids including peptide amphiphiles, and β-helical coiled-coil motifs.[8,9,84-90]

β-sheet peptides are widely used as self-assembled peptide motifs.[84] In pioneering work by Zhang et al., peptides of alternating hydrophilic and hydrophobic amino acid residues, Ac-$(AEAEAKAK)_2$-NH_2 (EAK16), which was originally found in a yeast protein zuotin, were self-assembled to form a hydrogel.[91] Similar types of amphipathic peptides such as Ac-$(FKFE)_2$-NH_2, Ac-$(RADA)_4$-NH_2, and QQKFQFQFEQQ (Q11) have been designed to form self-assembled nanofibers.[8] Based on the amphipathic peptides, we developed a C_3-symmetric "Wheel-FKFE" consisting of three FKFECKFE peptides connected to the arm of the C_3-symmetric core at the cysteine residue placed at the middle of the sequence, whose core and peptides can be considered to act as a hub and spokes of a wheel, respectively (Figure 7a).[92] Wheel-FKFE self-assembled to form nanofibers with a uniform width of 3–4 nm and lengths of several micrometers. The uniform width appears to be due to the columnar stacking of Wheel-FKFE by the formation of anti-parallel β-sheets.

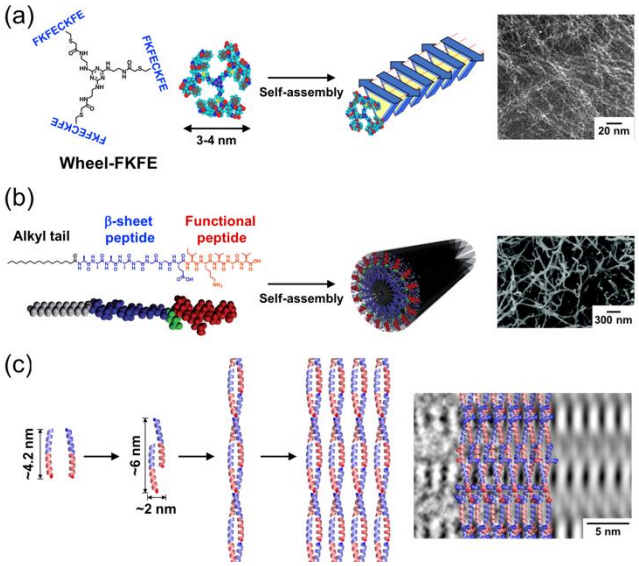

Figure 7. Design of self-assembled peptide-based nanofibers. (a) Self-assembly of Wheel-FKFE and TEM image. (b) Self-assembly of typical peptide amphiphile to form nanofibers and SEM image of IKVAV nanofiber. (c) Self-assembly of coiled-coil peptide fibers and high-resolution TEM images. Adapted with permission from refs. 92, 94, 96, and 100. Copyright 2008 American Chemical Society, 2004 American Association for the Advancement of Science, 2013 John Wiley and Sons, and 2012 National Academy of Sciences, U.S.A., respectively.

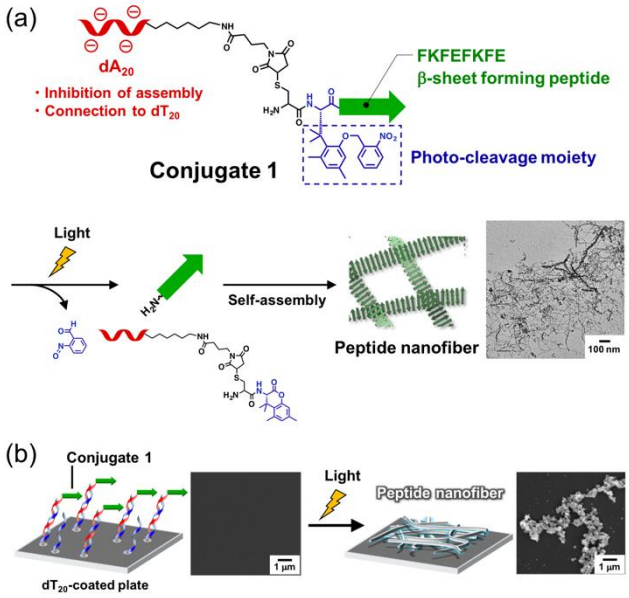

Figure 8. (a) Light-induced peptide nanofiber growth of conjugate **1** and TEM image of peptide nanofiber. (b) SEM images of conjugate **1** on dT_{20}-immobilized glass substrates before and after UV irradiation. Adapted with permission from ref. 123. Copyright 2015 Royal Society of Chemistry.

Peptide amphiphiles (PAs) consisting of a hydrophilic peptide sequence and a hydrophobic alkyl chain are also powerful building blocks to construct self-assembled nanofibers, which were developed by Stupp et al.[93-97] PAs are typically composed of a long alkyl tail, a β-sheet-forming peptide segment with a hydrophilic domain, and a functional peptide (Figure 7b). Self-assembly of PA is initiated by the formation of a micelle-like hydrophobic core by interaction of the alkyl tail; then, one-dimensional β-sheet formation by the proximal peptides facilitates nanofiber growth. By changing the outer functional peptides, PAs have been used for various applications such as cell culture,[94] regenerative medicines,[95,96] and growth of silver nanoparticles.[97]

Coiled-coil peptides are useful motifs for the rational design of self-assembling peptide nanofibers, as developed by Woolfson et al.[98-100] In their strategy, complementary 28-residue peptides were designed to form "sticky ends," which are parallel coiled-coil building blocks (2 × 6 nm) (Figure 7c). Association of the heterodimers at the overhanging ends affords self-assembly to form hexagonally packed fibers. The structures of the coiled-coil peptide fibers were determined at 8 Å resolution using cryo-TEM,[100] providing the structural insight for the design of peptide nanofibers.

3.2. Spatiotemporal Modulation of Peptide Nanofiber Growth

Formation/dissociation/morphological change of peptide nanofibers can be modulated by external stimuli such as enzymes,[80,81,101-108] redox,[108-115] temperature,[99,116] and light.[117-122] As a novel example, enzyme-triggered peptide nanofiber growth inside living cells has been developed for biomedical applications.[80,81] Generally, the strategy involves self-assembling peptides and enzyme-cleavable units connected as precursors. After being taken up by cells, these precursors are cleaved by intracellular enzymes and the released peptides self-assemble to form nanofibers, resulting in cell death[103-105] and intracellular targeting.[106,107] In addition, intracellular reductants such as glutathione and hydrogen sulfide can be used to trigger the formation of peptide nanofibers in living cells.[114,115] Among the external stimuli, light is particularly attractive because of the ease of manipulation with localized and on-demand irradiation. We developed a system of light-induced peptide nanofiber growth with spatiotemporal control by using peptide–DNA conjugates (Figure 8).[123] We synthesized conjugate **1** consisting of a β-sheet-forming FKFEFKFE peptide and an addressing single-stranded DNA (dA_{20}), which are linked by a photo-cleavable amino acid X (Figure 8a). Upon irradiation of UV light, conjugate **1** releases free FKFEFKFE peptide by the photocleavage reaction of X, which induces self-assembly of the peptide to form nanofibers 10–20 nm in width, as observed by TEM. Hybridization of conjugate **1** on the dT_{20}-immobilized glass plate was performed by complementary interaction of dA_{20} and dT_{20} for localized peptide nanofiber growth (Figure 8b). Although there were no obvious structures before UV irradiation (Figure 8b, left), UV irradiation induced the formation of micrometer-sized fibrillar structures (Figure 8b, right). In contrast, only small

amounts of microstructures of **1** were observed on the mismatched dA_{20}-immobilized glass substrate, even after UV irradiation. Thus, conjugate **1** can be immobilized at the specific site by DNA hybridization and the growth of the peptide nanofiber can be modulated by light.

3.3. Bioinspired Molecular Propulsion Based on Light-induced Peptide Nanofiber Growth

In nature, several bacterial pathogens utilize nanofiber growth for their self-propelled motility within cells. For instance, actin polymerization on the surface of *Listeria monocytogenes* was initiated by transmembrane protein ActA, resulting in a local network of actin filaments called an "actin comet tail", which provides a powerful force to propel the bacteria through the cytoplasm of host cells (Figure 9a).[124,125] Inspired by the natural fiber-induced propulsion, we created a light-induced propulsion system based on spatiotemporally controlled peptide nanofiber growth using peptide–DNA conjugates (Figure 9b).[126] In our design, a peptide nanofiber-forming unit (FKFEFKFE) with a photocleavage unit was asymmetrically conjugated on the surface of phase-separated giant liposomes via DNA hybridization of the addressing unit (dA_{20}). Upon UV light irradiation, the released peptide moieties around the liposomes self-assembled to form nanofibers, which could induce propulsion of the liposome by a mechanism similar to actin polymerization-induced motility. In addition to conjugate **1** used in the previous study,[123] conjugate **2**, which has a different photo-cleavable amino acid Z, was used (Figure 9c). Because Z is cleaved by light faster than X used in conjugate **1**, light-induced fiber formation of conjugate **2** was much faster than that of conjugate **1**. Conjugates **1** and **2** were asymmetrically modified on phase-separated giant liposomes by using dA_{20}–dT_{20} complementary hybridization and streptavidin–biotin interaction (**1-PS** and **2-PS**). Upon light irradiation to **2-PS**, the translational motion of **2-PS** was dramatically enhanced (Figure 9d). The velocity of **2-PS** was significantly higher than that of **1-PS**, indicating that the velocity reflects the rates of the photocleavage reaction and subsequent fiber formation of the peptide–DNA conjugates (Figure 9e). The design principle can be used to construct components of molecular robots that respond to the surrounding environment and make decisions autonomously.[127]

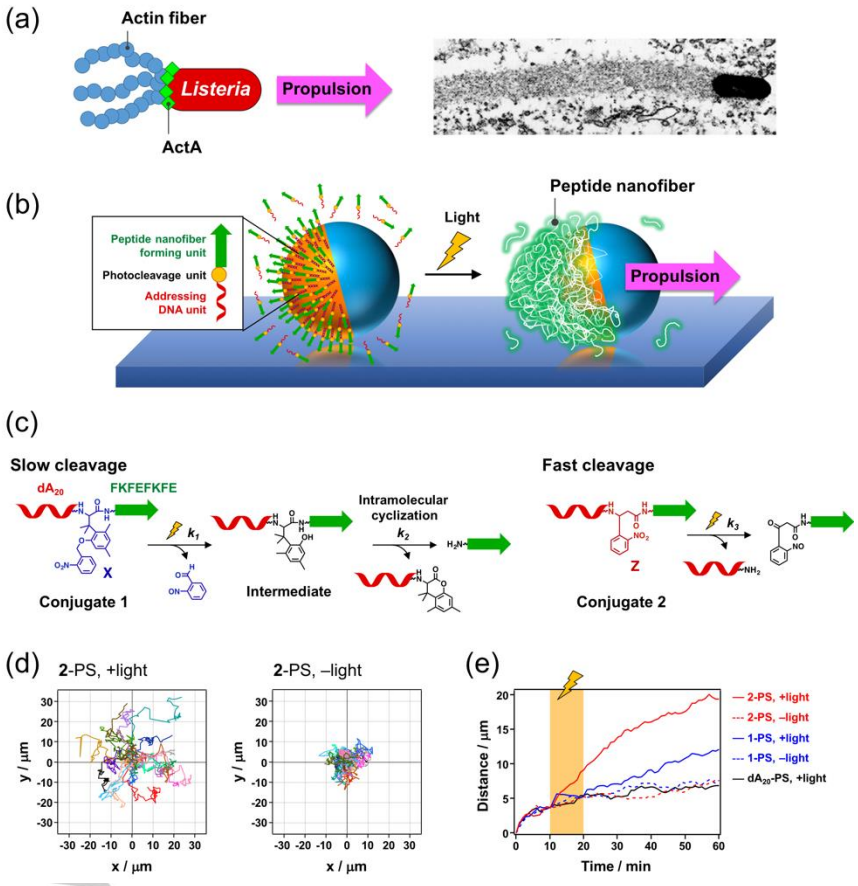

Figure 9. (a) Propulsion of *Listeria monocytogenes* driven by formation of actin fiber and TEM image. (b) Propulsion of a phase-separated (PS) giant liposome driven by light-induced peptide nanofiber growth using the peptide-DNA conjugates **1** and **2**. (c) Photocleavage reactions of conjugates **1** and **2**. (d) Tracking trajectories of **2**-conjugated PS liposome (**2**-PS) during 60 min with (left) and without (right) light irradiation. Irradiation lasted for 10–20 min of recording. (e) Average of time dependence of the distance of the PS-liposomes from the initial position under UV light irradiation (orange zones) and no irradiation (white zones). Adapted with permission from refs. 125 and 126. Copyright 1992 Elsevier and 2018 Springer Nature, respectively.

4. Protein-binding Peptides Designed from Natural Proteins

4.1. Protein-mimicking Peptides for Specific Binding to Target Proteins

Peptides are useful motifs that bind to their target proteins with high selectivity and affinity. Protein-binding peptides are useful not only for the structural and functional analysis of proteins, but also for therapeutic uses such as the inhibition of protein–protein interaction (PPI), signaling, cell adhesion, and protein tags.[22,23,128-131] One of the most well-known and simple examples is RGD peptide isolated from the adhesion protein fibronectin, which retains the cell-adhesive activity of fibronectin by binding to the integrin cell-surface receptors.[132] To design protein-binding peptides, various approaches have been developed, including isolation and design from natural proteins,[131,133-135] random screening such as phage display and peptide library method,[136,137] and *in silico* design.[138-140] The design of peptides that mimic the binding domains of natural proteins is a promising strategy to modulate the functions of target proteins. For instance, Vita et al. constructed peptides that mimic the binding site of a receptor (CD4) to a human immunodeficiency virus (HIV)-1 envelope glycoprotein (gp120) for the development of viral entry inhibitors (Figure 10a).[141,142] Since a CDR2-like loop of CD4 is a binding target of gp120 of HIV-1 in the initial step of viral entry into host cells, the solvent-exposed residues of the CDR2-like loop were transferred to the structurally homologous region of a scorpion toxin scaffold.[141] The CD4-mimicking peptide was further optimized by structural modeling based on information on the structure of the gp120–CD4 complex.[142] The optimized peptide was shown to have high binding affinity to gp120 variants with K_d values within the 1–20 nM range, which is comparable to that of native soluble recombinant CD4. The peptides inhibited the infection of various cell lines by HIV-1. Moreover, recently, a cyclic peptide was developed to inhibit sonic hedgehog (Shh) signaling, which plays an important role in embryonic development and cancer progression.[143] The cyclic peptide was designed based on the Shh-binding loop of hedgehog-interacting protein (HHIP), which is a membrane protein that acts as a negative regulator of the hedgehog pathway (Figure 10b). The screening of macrocyclic peptide libraries produced an optimized macrocyclic peptide with high binding affinity to Shh with a K_d of 170 nM, which is a 120-fold increase in affinity compared with that of the original linear peptide. One of the reasons for the high affinity of the macrocyclic peptide compared with the linear peptide is the conformational restriction, which results in reduced entropic cost upon binding to the target protein. The peptide effectively suppressed Shh-mediated hedgehog signaling and gene transcription. These examples clearly show that the two-step design, namely, isolation of protein-binding sites from natural proteins and subsequent optimization of the sequences by screening, is a promising strategy to construct protein-binding peptides with high affinity and selectivity to target proteins.

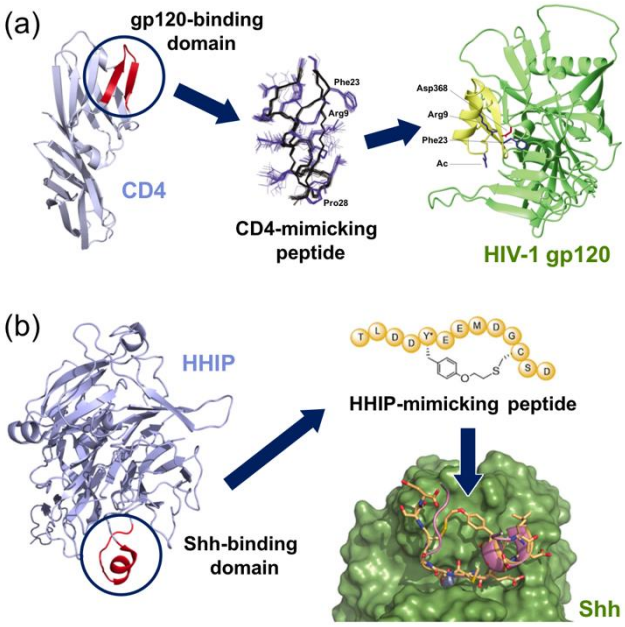

Figure 10. Design of protein-binding peptides from natural proteins. (a) CD4-mimicking peptide for binding to HIV-1 gp120 (PDB ID for CD4: 1CDH). (b) HHIP-mimicking macrocyclic peptide for binding to Shh (PDB ID for HHIP–Shh complex: 3HO5). Adapted with permission from refs. 142 and 143. Copyright 2003 Springer Nature and 2017 American Chemical Society, respectively.

4.2. Microtubule-binding Peptides for Molecular Encapsulation Inside Microtubules

Recently, we designed a microtubule-binding peptide from the natural microtubule-associated protein Tau in order to encapsulate functional molecules inside microtubules.[144] Microtubules are hollow tubular protein assemblies with an inner diameter of 15 nm and a length of several micrometers, which are composed of tubulin dimers (α- and β-tubulin). Based on the directional movement of a motor protein kinesin along the outer surface of microtubules, artificial molecular transport systems have been established for nanodevice applications.[145-149] Although the functionalization of the outer surface of microtubules has been established for nanomaterial applications, the inside of microtubules has received little attention. We designed peptides from the microtubule-binding region of Tau, which consists of imperfect repeat sequences (R1–R4) linked by interrepeat sequences (Figure 11a). Based on the repeat sequences, four Tau-derived peptides **1**$_N$, **1**$_C$, **2**$_N$, and **2**$_C$ were developed. All of the four tetramethylrhodamine (TMR)-labeled peptides were shown to bind to green fluorescent Alexa Fluor 430 (AF)-labeled microtubules. Among them, TMR-labeled **2**$_N$ (**2**$_N$**-TMR**) bound to the inside of microtubules by preincubation with tubulin and subsequent polymerization of the peptide–tubulin complex (Figure 11b). By conjugation of **2**$_N$ to AuNPs, encapsulation of the **2**$_N$-AuNP conjugates inside microtubules was achieved (Figure 11c). Preincubation of **2**$_N$-AuNPs with tubulin, subsequent polymerization, and treatment of anti-tubulin

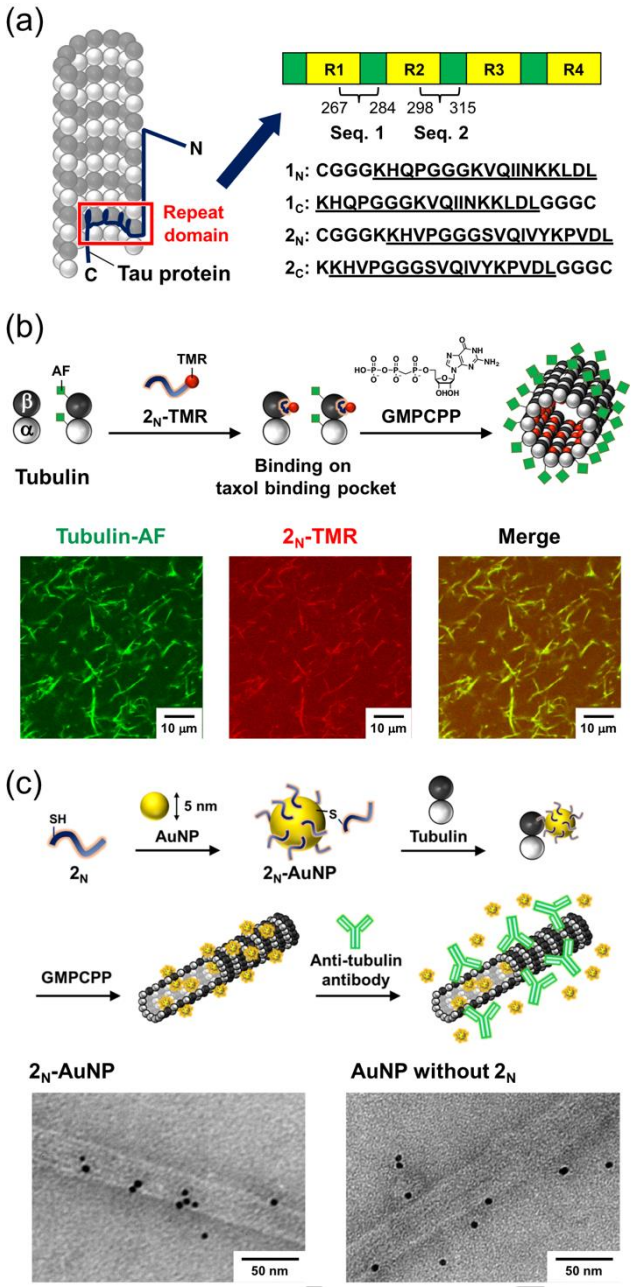

Figure 11. Molecular encapsulation into microtubule using Tau-derived peptides. (a) Design of the Tau-derived peptides $\mathbf{1}_N$, $\mathbf{1}_C$, $\mathbf{2}_N$, and $\mathbf{2}_C$ based on the binding repeats (R1, R2, R3, and R4) of Tau. The sequences **1** (267–284) and **2** (298–315) used in the Tau-derived peptides are underlined. (b) Encapsulation of TMR-labeled $\mathbf{2}_N$ ($\mathbf{2}_N$**-TMR**) into Alexa Fluor 430 (AF)-labeled microtubules (top). Confocal laser scanning microscopy (CLSM) images of microtubules incubated with $\mathbf{2}_N$**-TMR** (bottom). (c) Encapsulation of $\mathbf{2}_N$-AuNPs inside microtubules (top). TEM images of microtubules incubated with $\mathbf{2}_N$-AuNPs (bottom left) and unmodified AuNPs without $\mathbf{2}_N$ (bottom right). Adapted with permission from ref. 144. Copyright 2018 John Wiley and Sons.

antibody that binds to the outside of microtubules generated $\mathbf{2}_N$-AuNP-encapsulated microtubules. In contrast, when unmodified AuNPs without $\mathbf{2}_N$ were used, encapsulation of AuNPs inside microtubules was not observed. Thus, the Tau-derived peptide is useful to bind to the inside of microtubules for the encapsulation of nanomaterials. Combination of the peptide-based molecular encapsulation and the motility of microtubules should provide a new design concept for microtubule-based nanomaterials.

5. Summary and Outlook

In this account, we described recent progress in the peptide-based nanomaterials designed based on the natural supramolecular systems. First, peptide-based artificial viral capsids designed from the natural viral scaffolds were summarized. As a representative example, a β-annulus peptide extracted from the internal skeleton of TBSV was shown to self-assemble to form a spherical virus-like nanocapsule. Functional nanosized molecules such as metal nanoparticles, DNA, and proteins can be loaded to the inside and outside of β-annulus capsids. It is evident that one of the next steps of artificial viral capsids is to mimic the infectiousness of natural viruses. Synthetic viruses that can be delivered to target cells and release their cargo should be useful for gene and drug delivery applications while avoiding the barriers and regulations associated with the use of natural viruses. Second, design strategies of peptide nanofibers and our applications were described. The self-assembling ability of short peptide subunits is useful for the development of nanofibers with defined width. In the next generation, the formation, dissociation, and morphological change of peptide nanofibers were modulated by external stimuli such as enzymes, redox, temperature, and light. We reported the spatiotemporal modulation of peptide nanofiber growth based on peptide–DNA conjugates that are connected via photocleavage amino acids. We created a system of light-induced propulsion of giant liposomes based on the peptide–DNA conjugates by mimicking bacterial self-propelling systems. With regard to future work, if the formation and dissociation of peptide nanofibers in cells can be reversibly tuned by external stimuli, the “artificial cytoskeleton” should become a new concept for modulating the cell fate. Finally, the development of protein-binding peptides based on the partial domains of natural proteins was described. The extraction of protein-binding domains is a promising strategy for creating peptides that bind to target proteins with high selectivity and affinity. The application of protein-binding peptides has a versatile range of uses, such as inhibition of protein–protein interaction, cell adhesion, and protein tagging. We developed a Tau-derived peptide that specifically binds to the inside of microtubules, which is useful for encapsulating molecules inside microtubules. The characteristic property of peptides, recognition of target proteins, can be useful to target intracellular proteins to modulate cellular signaling, although there is a need to overcome several associated drawbacks, such as low cell permeability and short half-lives of peptides.

Peptides are excellent building blocks for the construction of nanomaterials because of the designability, self-assembly, molecular recognition ability, and ease of synthesis. Another

significant advantage is that peptides with desired structures and functions can be designed by mimicking natural supramolecular systems. In addition, the recent development of library screening methods has dramatically accelerated the exploration of optimized peptides with desired properties. One of the future directions of peptide-based nanomaterials is to mimic the dynamic functions of natural systems, such as motility, morphological change, and self-replication. The integration of different types of peptides and organic/inorganic materials should provide new design principles of complicated “molecular robots” as next-generation peptide nanomaterials beyond biological functions.

Acknowledgements

This work was supported by PRESTO, Japan Science and Technology Agency (JST), KAKENHI (No. 17K14517 for H. I. and 15H03838, 18H02089, 18H04558, 24104004 for K. M.) from the Japan Society for the Promotion of Science (JSPS).

Keywords: nanomaterials • peptides • self-assembly • artificial viral capsid • nanofiber • microtubules

[1] B. J. G. E. Pieters, M. B. van Eldijk, R. J. M. Nolte, J. Mecinović, *Chem. Soc. Rev.* **2016**, *45*, 24–39.
[2] A. L. Boyle, D. N. Woolfson, Rational Design of Peptide-Based Biosupramolecular Systems in *Supramolecular Chemistry: From Molecules to Nanomaterials* (Eds.: P. A. Gale, J. W. Steed), John Wiley and Sons, Hoboken, **2012**.
[3] *Peptide Materials: From Nanostructures to Applications* (Eds.: C. Alemán, A. Bianco, M. Venanzi), John Wiley and Sons, Hoboken, **2013**.
[4] *Self-Assembled Peptide Nanostructures: Advances and Applications in Nanobiotechnology* (Eds.: J. Castillo, L. Sasso, W. E. Svendsen), Pan Stanford Publishing, **2012**.
[5] C.-L. Chen, N. L. Rosi, *Angew. Chem. Int. Ed.* **2010**, *49*, 1924–1942.
[6] B. E. I. Ramakers, J. C. M. van Hest, D. W. P. M. Löwik, *Chem. Soc. Rev.* **2014**, *43*, 2743–2756.
[7] E. De Santis, M. G. Ryadnov, *Chem. Soc. Rev.* **2015**, *44*, 8288–8300.
[8] D. M. Raymond, B. L. Nilsson, *Chem. Soc. Rev.* **2018**, *47*, 3659–3720.
[9] H. Tsutsumi, H. Mihara, *Mol. Biosyst.* **2013**, *9*, 609–617.
[10] D. Mandal, A. Nasrolahi Shirazi, K. Parang, *Org. Biomol. Chem.* **2014**, *12*, 3544–3561.
[11] T. Sawada, H. Mihara, T. Serizawa, *Chem. Rec.* **2013**, *13*, 172–186.
[12] K. Matsuura, *RSC Adv.* **2014**, *4*, 2942–2953.
[13] K. Kinbara, T. Aida, *Chem. Rev.* **2005**, *105*, 1377–1400.
[14] Q. Luo, C. Hou, Y. Bai, R. Wang, J. Liu, *Chem. Rev.* **2016**, *116*, 13571–13632.
[15] F. Schwizer, Y. Okamoto, T. Heinisch, Y. Gu, M. M. Pellizzoni, V. Lebrun, R. Reuter, V. Köhler, J. C. Lewis, T. R. Ward, *Chem. Rev.* **2018**, *118*, 142–231.
[16] F. A. Aldaye, A. L. Palmer, H. F. Sleiman, *Science* **2008**, *321*, 1795–1799.
[17] O. I. Wilner, I. Willner, *Chem. Rev.* **2012**, *112*, 2528–2556.
[18] M. R. Jones, N. C. Seeman, C. A. Mirkin, *Science* **2015**, *347*, 1260901.
[19] A. Samanta, I. L. Medintz, *Nanoscale* **2016**, *8*, 9037–9095.
[20] Q. Hu, H. Li, L. Wang, H. Gu, C. Fan, *Chem. Rev.* **2018**, DOI 10.1021/acs.chemrev.7b00663.
[21] T. R. Walsh, M. R. Knecht, *Chem. Rev.* **2017**, *117*, 12641–12704.
[22] I. W. Hamley, *Chem. Rev.* **2017**, *117*, 14015–14041.
[23] M. Pelay-Gimeno, A. Glas, O. Koch, T. N. Grossmann, *Angew. Chem. Int. Ed.* **2015**, *54*, 8896–8927.
[24] D. W. P. M. Löwik, E. H. P. Leunissen, M. van den Heuvel, M. B. Hansen, J. C. M. Van Hest, *Chem. Soc. Rev.* **2010**, *39*, 3394–3412.
[25] O. Zozulia, M. A. Dolan, I. V. Korendovych, *Chem. Soc. Rev.* **2018**, *47*, 3621–3639.
[26] T. Douglas, M. Young, *Nature* **1998**, *393*, 152–155.
[27] T. Douglas, M. Young, *Science* **2006**, *312*, 873–875.
[28] N. F. Steinmetz, D. J. Evans, *Org. Biomol. Chem.* **2007**, *5*, 2891–2902.
[29] L. M. Bronstein, *Small* **2011**, *7*, 1609–1618.
[30] L. S. Witus, M. B. Francis, *Acc. Chem. Res.* **2011**, *44*, 774–783.
[31] Z. Liu, J. Qiao, Z. Niu, Q. Wang, *Chem. Soc. Rev.* **2012**, *41*, 6178–6194.
[32] F. Li, Q. Wang, *Small* **2013**, *10*, 230–245.
[33] A. M. Wen, N. F. Steinmetz, *Chem. Soc. Rev.* **2016**, *45*, 4074–4126.
[34] H. Inaba, T. Ueno, *Biophys. Rev.* **2018**, *10*, 641–658.
[35] H. Inaba, S. Kitagawa, T. Ueno, *Isr. J. Chem.* **2014**, *55*, 40–50.
[36] B. Maity, K. Fujita, T. Ueno, *Curr. Opin. Chem. Biol.* **2015**, *25*, 88–97.
[37] E. Busseron, Y. Ruff, E. Moulin, N. Giuseppone, *Nanoscale* **2013**, *5*, 7098–7140.
[38] L. Zhang, L. H. L. Lua, A. P. J. Middelberg, Y. Sun, N. K. Connors, *Chem. Soc. Rev.* **2015**, *44*, 8608–8618.
[39] K. Matsuura, *Polym. J.* **2012**, *44*, 469–474.
[40] K. Matsuura, *Chem. Commun.* **2018**, *54*, 8944–8959.
[41] N. Kawakami, H. Kondo, Y. Matsuzawa, K. Hayasaka, E. Nasu, K. Sasahara, R. Arai, K. Miyamoto, *Angew. Chem. Int. Ed.* **2018**, *57*, 12400–12404.
[42] N. P. King, J. B. Bale, W. Sheffler, D. E. McNamara, S. Gonen, T. Gonen, T. O. Yeates, D. Baker, *Nature* **2014**, *510*, 103–108.
[43] N. P. King, W. Sheffler, M. R. Sawaya, B. S. Vollmar, J. P. Sumida, I. André, T. Gonen, T. O. Yeates, D. Baker, *Science* **2012**, *336*, 1171–1174.
[44] J. B. Bale, S. Gonen, Y. Liu, W. Sheffler, D. Ellis, C. Thomas, D. Cascio, T. O. Yeates, T. Gonen, N. P. King, D. Baker, *Science* **2016**, *353*, 389–394.
[45] Y. Hsia, J. B. Bale, S. Gonen, D. Shi, W. Sheffler, K. K. Fong, U. Nattermann, C. Xu, P.-S. Huang, R. Ravichandran, S. Yi, T. N. Davis, T. Gonen, N. P. King, D. Baker, *Nature* **2016**, *535*, 136–139.
[46] K. Matsuura, K. Murasato, N. Kimizuka, *J. Am. Chem. Soc.* **2005**, *127*, 10148–10149.
[47] K. Matsuura, H. Hayashi, K. Murasato, N. Kimizuka, *Chem. Commun.* **2011**, *47*, 265–267.
[48] K. Matsuura, H. Matsuyama, T. Fukuda, T. Teramoto, K. Watanabe, K. Murasato, N. Kimizuka, *Soft Matter* **2009**, *5*, 2463–2470.
[49] K. Matsuura, K. Tochio, K. Watanabe, N. Kimizuka, *Chem. Lett.* **2011**, *40*, 711–713.
[50] K. Matsuura, K. Fujino, T. Teramoto, K. Murasato, *Bull. Chem. Soc. Jpn.* **2010**, *83*, 880–886.
[51] S. Ghosh, M. Reches, E. Gazit, S. Verma, *Angew. Chem. Int. Ed.* **2007**, *46*, 2002–2004.
[52] V. Castelletto, E. De Santis, H. Alkassem, B. Lamarre, J. E. Noble, S. Ray, A. Bella, J. R. Burns, B. W. Hoogenboom, M. G. Ryadnov, *Chem. Sci.* **2016**, *7*, 1707–1711.
[53] R. J. Brea, N. K. Devaraj, *Nat. Commun.* **2017**, *8*, 730.
[54] K. Matsuura, K. Watanabe, T. Matsuzaki, K. Sakurai, N. Kimizuka, *Angew. Chem. Int. Ed.* **2010**, *49*, 9662–9665.
[55] K. Matsuura, Y. Mizuguchi, N. Kimizuka, *Biopolymers* **2016**, *106*, 470–475.
[56] A. J. Olson, G. Bricogne, S. C. Harrison, *J. Mol. Biol.* **1983**, *171*, 61–93.
[57] S. C. Harrison, A. J. Olson, C. E. Schutt, F. K. Winkler, G. Bricogne, *Nature* **1978**, *276*, 368–373.
[58] C. Hsu, P. Singh, W. Ochoa, D. J. Manayani, M. Manchester, A. Schneemann, V. S. Reddy, *Virology* **2006**, *349*, 222–229.
[59] K. Matsuura, K. Watanabe, Y. Matsushita, N. Kimizuka, *Polym. J.* **2013**, *45*, 529–534.

[60] S. Fujita, K. Matsuura, *Chem. Lett.* **2016**, *45*, 922–924.
[61] S. Fujita, K. Matsuura, *Nanomaterials* **2014**, *4*, 778–791.
[62] K. Matsuura, T. Nakamura, K. Watanabe, T. Noguchi, K. Minamihata, N. Kamiya, N. Kimizuka, *Org. Biomol. Chem.* **2016**, *14*, 7869–7874.
[63] K. Matsuura, G. Ueno, S. Fujita, *Polym. J.* **2015**, *47*, 146–151.
[64] Y. Nakamura, S. Yamada, S. Nishikawa, K. Matsuura, *J. Pept. Sci.* **2017**, *23*, 636–643.
[65] S. Fujita, K. Matsuura, *Org. Biomol. Chem.* **2017**, *15*, 5070–5077.
[66] S. G. Tarasov, V. Gaponenko, O. M. Z. Howard, Y. Chen, J. J. Oppenheim, M. A. Dyba, S. Subramaniam, Y. Lee, C. Michejda, N. I. Tarasova, *Proc. Natl. Acad. Sci. U.S.A.* **2011**, *108*, 9798–9803.
[67] F. Lapenta, J. Aupič, Ž. Strmšek, R. Jerala, *Chem. Soc. Rev.* **2018**, *47*, 3530–3542.
[68] M. G. Ryadnov, *Angew. Chem. Int. Ed.* **2007**, *46*, 969–972.
[69] J. M. Fletcher, R. L. Harniman, F. R. H. Barnes, A. L. Boyle, A. Collins, J. Mantell, T. H. Sharp, M. Antognozzi, P. J. Booth, N. Linden, M. J. Miles, R. B. Sessions, P. Verkade, D. N. Woolfson, *Science* **2013**, *340*, 595–599.
[70] E. De Santis, H. Alkassem, B. Lamarre, N. Faruqui, A. Bella, J. E. Noble, N. Micale, S. Ray, J. R. Burns, A. R. Yon, B. W. Hoogenboom, M. G. Ryadnov, *Nat. Commun.* **2017**, *8*, 2263.
[71] J. E. Noble, E. De Santis, J. Ravi, B. Lamarre, V. Castelletto, J. Mantell, S. Ray, M. G. Ryadnov, *J. Am. Chem. Soc.* **2016**, *138*, 12202–12210.
[72] Y. Ruff, T. Moyer, C. J. Newcomb, B. Demeler, S. I. Stupp, *J. Am. Chem. Soc.* **2013**, *135*, 6211–6219.
[73] G. Grigoryan, Y. H. Kim, R. Acharya, K. Axelrod, R. M. Jain, L. Willis, M. Drndic, J. M. Kikkawa, W. F. DeGrado, *Science* **2011**, *332*, 1071–1076.
[74] G. Wei, Z. Su, N. P. Reynolds, P. Arosio, I. W. Hamley, E. Gazit, R. Mezzenga, *Chem. Soc. Rev.* **2017**, *46*, 4661–4708.
[75] J. H. Collier, J. S. Rudra, J. Z. Gasiorowski, J. P. Jung, *Chem. Soc. Rev.* **2010**, *39*, 3413–3424.
[76] J. B. Matson, S. I. Stupp, *Chem. Commun.* **2012**, *48*, 26–33.
[77] H. Cui, M. J. Webber, S. I. Stupp, *Biopolymers* **2010**, *94*, 1–18.
[78] J. Zhou, J. Li, X. Du, B. Xu, *Biomaterials* **2017**, *129*, 1–27.
[79] Y. Loo, S. Zhang, C. A. E. Hauser, *Biotechnol. Adv.* **2012**, *30*, 593–603.
[80] H. Acar, S. Srivastava, E. J. Chung, M. R. Schnorenberg, J. C. Barrett, J. L. LaBelle, M. Tirrell, *Adv. Drug Deliv. Rev.* **2017**, *110-111*, 65–79.
[81] H. Wang, Z. Feng, B. Xu, *Chem. Soc. Rev.* **2017**, *46*, 2421–2436.
[82] A. Dasgupta, J. H. Mondal, D. Das, *RSC Adv.* **2013**, *3*, 9117–9149.
[83] X. Du, J. Zhou, J. Shi, B. Xu, *Chem. Rev.* **2015**, *115*, 13165–13307.
[84] L. M. De Leon Rodriguez, Y. Hemar, J. Cornish, M. A. Brimble, *Chem. Soc. Rev.* **2016**, *45*, 4797–4824.
[85] C. A. E. Hauser, S. Zhang, *Chem. Soc. Rev.* **2010**, *39*, 2780–2790.
[86] I. W. Hamley, *Angew. Chem. Int. Ed.* **2007**, *46*, 8128–8147.
[87] D. N. Woolfson, Z. N. Mahmoud, *Chem. Soc. Rev.* **2010**, *39*, 3464–3479.
[88] D. N. Woolfson, M. G. Ryadnov, *Curr. Opin. Chem. Biol.* **2006**, *10*, 559–567.
[89] J. Sato, T. Takahashi, H. Oshima, S. Matsumura, H. Mihara, *Chem. Eur. J.* **2007**, *13*, 7745–7752.
[90] T. P. J. Knowles, M. J. Buehler, *Nat. Nanotechnol.* **2011**, *6*, 469–479.
[91] S. Zhang, T. Holmes, C. Lockshin, A. Rich, *Proc. Natl. Acad. Sci. U.S.A.* **1993**, *90*, 3334–3338.
[92] K. Murasato, K. Matsuura, N. Kimizuka, *Biomacromolecules* **2008**, *9*, 913–918.
[93] J. D. Hartgerink, E. Beniash, S. I. Stupp, *Science* **2001**, *294*, 1684–1688.
[94] G. A. Silva, C. Czeisler, K. L. Niece, E. Beniash, D. A. Harrington, J. A. Kessler, S. I. Stupp, *Science* **2004**, *303*, 1352–1355.
[95] M. P. Hendricks, K. Sato, L. C. Palmer, S. I. Stupp, *Acc. Chem. Res.* **2017**, *50*, 2440–2448.
[96] M. J. Webber, E. J. Berns, S. I. Stupp, *Isr. J. Chem.* **2013**, *53*, 530–554.
[97] E. Pazos, E. Sleep, C. M. Rubert Pérez, S. S. Lee, F. Tantakitti, S. I. Stupp, *J. Am. Chem. Soc.* **2016**, *138*, 5507–5510.
[98] D. Papapostolou, A. M. Smith, E. D. T. Atkins, S. J. Oliver, M. G. Ryadnov, L. C. Serpell, D. N. Woolfson, *Proc. Natl. Acad. Sci. U.S.A.* **2007**, *104*, 10853–10858.
[99] E. F. Banwell, E. S. Abelardo, D. J. Adams, M. A. Birchall, A. Corrigan, A. M. Donald, M. Kirkland, L. C. Serpell, M. F. Butler, D. N. Woolfson, *Nat. Mater.* **2009**, *8*, 596–600.
[100] T. H. Sharp, M. Bruning, J. Mantell, R. B. Sessions, A. R. Thomson, N. R. Zaccai, R. L. Brady, P. Verkade, D. N. Woolfson, *Proc. Natl. Acad. Sci. U.S.A.* **2012**, *109*, 13266–13271.
[101] D. Koda, T. Maruyama, N. Minakuchi, K. Nakashima, M. Goto, *Chem. Commun.* **2010**, *46*, 979–981.
[102] Y. Gao, J. Shi, D. Yuan, B. Xu, *Nat. Commun.* **2012**, *3*, 1033.
[103] A. Tanaka, Y. Fukuoka, Y. Morimoto, T. Honjo, D. Koda, M. Goto, T. Maruyama, *J. Am. Chem. Soc.* **2015**, *137*, 770–775.
[104] Z. Yang, G. Liang, Z. Guo, Z. Guo, B. Xu, *Angew. Chem. Int. Ed.* **2007**, *46*, 8216–8219.
[105] Z. M. Yang, K. M. Xu, Z. F. Guo, Z. H. Guo, B. Xu, *Adv. Mater.* **2007**, *19*, 3152–3156.
[106] H. He, J. Wang, H. Wang, N. Zhou, D. Yang, D. R. Green, B. Xu, *J. Am. Chem. Soc.* **2018**, *140*, 1215–1218.
[107] J. Li, Y. Kuang, J. Shi, J. Zhou, J. E. Medina, R. Zhou, D. Yuan, C. Yang, H. Wang, Z. Yang, J. Liu, D. M. Dinulescu, B. Xu, *Angew. Chem. Int. Ed.* **2015**, *54*, 13307–13311.
[108] Z. Zheng, P. Chen, M. Xie, C. Wu, Y. Luo, W. Wang, J. Jiang, G. Liang, *J. Am. Chem. Soc.* **2016**, *138*, 11128–11131.
[109] C. J. Bowerman, B. L. Nilsson, *J. Am. Chem. Soc.* **2010**, *132*, 9526–9527.
[110] X. Li, J. Li, Y. Gao, Y. Kuang, J. Shi, B. Xu, *J. Am. Chem. Soc.* **2010**, *132*, 17707–17709.
[111] M. Ikeda, T. Tanida, T. Yoshii, I. Hamachi, *Adv. Mater.* **2011**, *23*, 2819–2822.
[112] Y. Zhang, B. Zhang, Y. Kuang, Y. Gao, J. Shi, X. X. Zhang, B. Xu, *J. Am. Chem. Soc.* **2013**, *135*, 5008–5011.
[113] W. Wang, G. Li, W. Zhang, J. Gao, J. Zhang, C. Li, D. Ding, D. Kong, *RSC Adv.* **2014**, *4*, 30168–30171.
[114] S. Wei, X.-R. Zhou, Z. Huang, Q. Yao, Y. Gao, *Chem. Commun.* **2018**, *54*, 9051–9054.
[115] J. Zhan, Y. Cai, S. He, L. Wang, Z. Yang, *Angew. Chem. Int. Ed.* **2018**, *57*, 1813–1816.
[116] D. J. Pochan, J. P. Schneider, J. Kretsinger, B. Ozbas, K. Rajagopal, L. Haines, *J. Am. Chem. Soc.* **2003**, *125*, 11802–11803.
[117] C. J. Bosques, B. Imperiali, *J. Am. Chem. Soc.* **2003**, *125*, 7530–7531.
[118] L. A. Haines, K. Rajagopal, B. Ozbas, D. A. Salick, D. J. Pochan, J. P. Schneider, *J. Am. Chem. Soc.* **2005**, *127*, 17025–17029.
[119] Y. Matsuzawa, K. Ueki, M. Yoshida, N. Tamaoki, T. Nakamura, H. Sakai, M. Abe, *Adv. Funct. Mater.* **2007**, *17*, 1507–1514.
[120] Z. Qiu, H. Yu, J. Li, Y. Wang, Y. Zhang, *Chem. Commun.* **2009**, 3342–3344.
[121] T. Muraoka, H. Cui, S. I. Stupp, *J. Am. Chem. Soc.* **2008**, *130*, 2946–2947.
[122] T. Muraoka, C.-Y. Koh, H. Cui, S. I. Stupp, *Angew. Chem. Int. Ed.* **2009**, *48*, 5946–5949.
[123] M. Furutani, A. Uemura, A. Shigenaga, C. Komiya, A. Otaka, K. Matsuura, *Chem. Commun.* **2015**, *51*, 8020–8022.
[124] A. Upadhyaya, A. van Oudenaarden, *Curr. Biol.* **2003**, *13*, R734–R744.
[125] C. Kocks, E. Gouin, M. Tabouret, P. Berche, H. Ohayon, P. Cossart, *Cell* **1992**, *68*, 521–531.
[126] H. Inaba, A. Uemura, K. Morishita, T. Kohiki, A. Shigenaga, A. Otaka, K. Matsuura, *Sci. Rep.* **2018**, *8*, 6243.
[127] M. Hagiya, A. Konagaya, S. Kobayashi, H. Saito, S. Murata, *Acc. Chem. Res.* **2014**, *47*, 1681–1690.
[128] L. Nevola, E. Giralt, *Chem. Commun.* **2015**, *51*, 3302–3315.
[129] P. Wójcik, Ł. Berlicki, *Bioorg. Med. Chem. Lett.* **2016**, *26*, 707–713.
[130] L.-G. Milroy, T. N. Grossmann, S. Hennig, L. Brunsveld, C. Ottmann, *Chem. Rev.* **2014**, *114*, 4695–4748.

[131] F. Iavarone, C. Desiderio, A. Vitali, I. Messana, C. Martelli, M. Castagnola, T. Cabras, *Crit. Rev. Biochem. Mol. Biol.* **2018**, *53*, 246–263.
[132] M. D. Pierschbacher, E. Ruoslahti, *Nature* **1984**, *309*, 30–33.
[133] J. A. Robinson, S. DeMarco, F. Gombert, K. Moehle, D. Obrecht, *Drug Discov. Today* **2008**, *13*, 944–951.
[134] A. Groß, C. Hashimoto, H. Sticht, J. Eichler, *Front. Bioeng. Biotechnol.* **2016**, *3*, 211.
[135] D. J. Autelitano, A. Rajic, A. I. Smith, M. C. Berndt, L. L. Ilag, M. Vadas, *Drug Discov. Today* **2006**, *11*, 306–314.
[136] C.-H. Wu, I.-J. Liu, R.-M. Lu, H.-C. Wu, *J. Biomed. Sci.* **2016**, *23*, 8.
[137] N. K. Bashiruddin, H. Suga, *Curr. Opin. Chem. Biol.* **2015**, *24*, 131–138.
[138] P. Vanhee, A. M. van der Sloot, E. Verschueren, L. Serrano, F. Rousseau, J. Schymkowitz, *Trends Biotechnol.* **2011**, *29*, 231–239.
[139] S.-H. Wang, J. Yu, *Biomaterials* **2018**, *156*, 1–15.
[140] H. Yin, J. S. Slusky, B. W. Berger, R. S. Walters, G. Vilaire, R. I. Litvinov, J. D. Lear, G. A. Caputo, J. S. Bennett, W. F. DeGrado, *Science* **2007**, *315*, 1817–1822.
[141] C. Vita, E. Drakopoulou, J. Vizzavona, S. Rochette, L. Martin, A. Ménez, C. Roumestand, Y. S. Yang, L. Ylisastigui, A. Benjouad, J. C. Gluckman, *Proc. Natl. Acad. Sci. U.S.A.* **1999**, *96*, 13091–13096.
[142] L. Martin, F. Stricher, D. Missé, F. Sironi, M. Pugnière, P. Barthe, R. Prado-Gotor, I. Freulon, X. Magne, C. Roumestand, A. Ménez, P. Lusso, F. Veas, C. Vita, *Nat. Biotechnol.* **2003**, *21*, 71–76.
[143] A. E. Owens, I. de Paola, W. A. Hansen, Y.-W. Liu, S. D. Khare, R. Fasan, *J. Am. Chem. Soc.* **2017**, *139*, 12559–12568.
[144] H. Inaba, T. Yamamoto, A. M. R. Kabir, A. Kakugo, K. Sada, K. Matsuura, *Chem. Eur. J.* **2018**, DOI 10.1002/chem.201802617.
[145] H. Hess, J. L. Ross, *Chem. Soc. Rev.* **2017**, *46*, 5570–5587.
[146] G. D. Bachand, E. D. Spoerke, M. J. Stevens, *Biotechnol. Bioeng.* **2015**, *112*, 1065–1073.
[147] N. Isozaki, H. Shintaku, H. Kotera, T. L. Hawkins, J. L. Ross, R. Yokokawa, *Sci. Rob.* **2017**, *2*, eaan4882.
[148] J. J. Keya, R. Suzuki, A. M. R. Kabir, D. Inoue, H. Asanuma, K. Sada, H. Hess, A. Kuzuya, A. Kakugo, *Nat. Commun.* **2018**, *9*, 453.
[149] J. J. Keya, A. M. R. Kabir, D. Inoue, K. Sada, H. Hess, A. Kuzuya, A. Kakugo, *Sci. Rep.* **2018**, *8*, 11756.

Entry for the Table of Contents

PERSONAL ACCOUNT

Natural supramolecular assemblies possess characteristic properties that have developed over the course of evolution. By mimicking natural systems, various bio-nanomaterials have been constructed. This personal account describes our recent progress in the construction of peptide-based nanomaterials designed from the intrinsic functions of natural supramolecular systems.

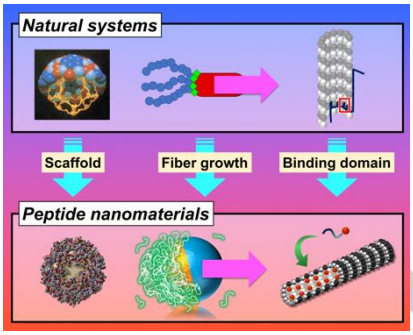

*Hiroshi Inaba and Kazunori Matsuura**

Page No. – Page No.

Peptide Nanomaterials Designed from Natural Supramolecular Systems